Mesoporous silica as a carrier for topical application: the Trolox case study

UNIVERSITÀ DEGLI STUDI DI TORINO

Mesoporous silica as a carrier for topical application: the Trolox case study

L. Gastaldi, E. Ugazio, S. Sapino, P. Iliade, I. Miletto, G. Berlier

Physical Chemistry Chemical Physics, 14 (2012) 11318–11326.

DOI:10.1039/C2CP41351E.

Mesoporous silica as a carrier for topical application: the Trolox case study

L. Gastaldi[1], E. Ugazio[1], S. Sapino[1], P. Iliade[2], I. Miletto[2], G. Berlier[21]

[1] University of Turin, Dipartimento di Scienza e Tecnologia del Farmaco, via P. Giuria 9, 10125 Torino, Italy.

[2] University of Turin, Dipartimento di Chimica and NIS, Nanostructured Interfaces and Surfaces Centre of Excellence, via P. Giuria 7, 10125 Torino, Italy.

[1] Corresponding author: e-mail: gloria.berlier@unito.it, Phone: +39-011-670-7856; Fax: +39-011-670-7953

Abstract

As part of a recent research effort aimed at employing mesoporous materials for controlled drug delivery, this paper presents MCM-41 as a carrier for topical application, using Trolox as a model unstable guest molecule. The complexes between Trolox and MCM-41 were prepared by employing different inclusion procedures, varying solvent, method and pretreatment of the silica matrix. The objectives of this study were to determine Trolox loading, analyze its integrity and availability after immobilization on mesoporous silica, evaluate MCM-41 influence on Trolox photodegradation and establish whether preparation method significantly influences complex properties. The characterization analyses (XRD, TGA, DSC, and FTIR) confirmed the hydrogen-bonding interaction and Trolox structure preservation. Gas-volumetric analysis showed a consistent decrease in surface area and in pore volume and diameter with respect to bare MCM-41 indicating that Trolox was mainly located within mesopores. *In vitro* diffusion tests showed a slower release of Trolox after inclusion in the MCM-41 matrix; at the same time UV irradiation studies highlighted an increased photostability for the complex particularly in O/W emulsion. Moreover the radical scavenging activity of Trolox was maintained after immobilization. In all cases, differences were observed in all tested samples, suggesting that results could be optimized by modifying the inclusion procedure and by improving the guest loading.

Keywords

Trolox, ordered mesoporous silica, immobilization, photostability, emulsion

1. Introduction

Trolox, a water soluble derivative of vitamin E, has been extensively investigated due to its antioxidant properties: it is widely used as a standard antioxidant in biochemical studies to assess the role of oxidative injury in processes like cell death and ageing.[1,2] The interesting and wide

applications of Trolox are due to its molecular structure (scheme 1): its carboxylic group confers a good water solubility while the presence of phenolic functionality is responsible for a series of properties. As a matter of fact, phenolic compounds have been demonstrated to reduce atherosclerosis, coronary heart disease, various cancer types and several dermal disorders.[3] The addition of Trolox proved extremely effective in reducing the cytotoxicity induced by UV irradiation.[4]

Many antioxidants, commonly used in cosmetic and pharmaceutical products, are known to become unstable upon UV irradiation, so that the topical administration of these molecules is restricted by their fast photodegradation. Likewise, Trolox can undergo photo-destabilization producing the intermediate Trolox-C-quinone, so new strategies must be found to improve its stability thus enhancing its use in pharmaceutical field.[5,6] To these aims, a recently proposed approach consists in the inclusion in supramolecular structures as phospholipid pockets, cyclodextrin cage holes,[7-9] or inorganic matrices such as hydrotalcite layered structures,[10,11] or mesoporous silica materials.[12-16]

MCM-41 mesoporous silica is a promising candidate for the vehiculation of compounds in pharmaceutical formulations, thanks to the well known properties, namely high surface area (around 1000 m^2g^{-1}), tunable pores dimensions (20-40 nm), uniform porous structure, thermal stability and biocompatibility.[17] Due to stable mesoporous structure and well-defined surface properties, mesoporous materials seem ideal for encapsulation of drugs, proteins and other biogenic molecules.[18-21] Organic molecules can be physically adsorbed (and thus easily released) within the silica pores through hydrogen bonding with surface Si-OH groups. Moreover, the silica surface can be functionalized by covalent anchoring of organic groups, thus modifying the material hydrophobicity/hydrophilicity and surface chemistry and improving the host/guest interaction.[22]

In this work, we report on the preparation and properties of Trolox/MCM-41 complexes, designed to incorporate Trolox molecules inside the hexagonal porous structure which acts as a vehicle and reduce photodegradation of the active ingredient. Different methods and conditions

(solvent nature and polarity, loading procedure) were employed to optimize drug immobilization and inclusion efficiency. The resulting complexes were characterized about their physico-chemical properties and tested for the influence of the host on release. Finally, one of the sample was selected, on the basis of a good compromise among loading, release rate and Trolox molecular dispersion, and tested about photostability and antiradical performance of the guest molecule.

2. Experimental section

2.1 Samples preparation

2.1.1 MCM-41 synthesis

Purely siliceous mesoporous MCM-41 was synthesized according to literature using SiO_2 in basic conditions and cetyltrimethylammonium bromide (CTAB, Aldrich) as structure directing agent (SDA).[23,24] After a hydrothermal treatment in autoclave, the resulting white product was filtered, washed with abundant distilled water, dried in oven at 100 °C for one night and finally calcined in nitrogen and oxygen atmosphere at 550 °C.

2.1.2 Trolox storage

Four procedures were followed to prepare inclusion complexes based on Trolox (6-hydroxy-2,5,7,8-tetramethylchromane-2-carboxylic acid, 97%, Aldrich) and MCM-41.

According to the impregnation method, firstly MCM-41 (400.0 mg) was added to aqueous suspension of Trolox (100.0 mg in 100.0 ml of filtered water); secondly 500.0 mg MCM-41 were added to 5.0 ml of 100.0 mg/ml Trolox methanol solution; thirdly the same 1/1 w/w ratio was employed using MCM-41 outgassed at 150 °C for 2 h to remove the adsorbed water. In all cases the mixtures were kept under magnetic stirring at room temperature (RT) for 24 h and after centrifugation the precipitate was dried under vacuum. The resulting materials are hereafter labeled as T/MCM-41/W, T/MCM-41/M and T/MCM-41/DEG, respectively.

Eventually, the kneading method was employed to prepare a 1/2 weight ratio Trolox/MCM-41 complexes.[25] A homogeneous paste of Trolox was prepared by mixing 30.0 mg Trolox with 250.0 µl of acetone in a mortar. 60.0 mg of MCM-41 were added to Trolox paste and the mixture was kneaded until acetone complete evaporation (about 10 min). The sample, hereafter named T/MCM-41/DRY, was then dried under vacuum.

Trolox loading was spectrophotometrically determined working at a wavelength of 290 nm after extraction with absolute methanol according to the procedure described below. Each quantified datum was averaged from triplicate analysis. Based on the final loading of drug in the complexes, a physical mixture was prepared as a reference, by mixing in a mortar Trolox and MCM-41 in a 1/4 weight ratio.

2.1.3 Trolox analysis

UV-Vis analysis of Trolox was performed in absolute methanol with an UV-Vis spectrophotometer DU 730 (Beckman Coulter). The Trolox calibration curve was determined by plotting absorbance *vs* Trolox concentration between 3.5×10^{-5} and 2.5×10^{-4} M. For this interval, the calibration curve fits the Lambert and Beers' law:

$$A = 3603.3 \times C \quad (R^2 = 0.9995)$$

where A is the absorbance and C is the molar concentration (M).

HPLC analysis was performed employing an apparatus (Shimadzu) consisting of a LC-6A pump unit control, a SPD-2A UV-Vis detector, a C-R3A chromatopac integrator and a RP-C18 column (Waters, 150×4.6 mm; 5 µm). Trolox was eluted with a mixture of methanol/water/HCl (55.0/45.0/0.4 v/v/v) and its flow rate was kept at 0.8 ml/min. The amount of Trolox in the samples was quantified, based on the standard curve generated by calculating HPLC peak area of pure Trolox.

2.2. Characterization methods

2.2.1 XRD

Powder X ray diffractions (XRD) patterns were collected on a X'Pert Pro Bragg Brentano diffractometer (Philips) using Cu Kα radiation (40 mA and 45 kV), with a scan speed of 0.01° min^{-1}.

2.2.2 Thermo-gravimetric analysis

A thermo-gravimetric analysis (TGA) was carried out on a TAQ600 (TA Instruments) heating the samples at a rate of 10 °C min^{-1} from 30 to 1000 °C in a nitrogen flow. Before starting the measurements, samples were equilibrated at 30 °C. Once reached the final temperature an isotherm was run for 15 min in air, to burn carbonaceous residues from pyrolysis reactions and measure the total organic amount.

2.2.3 Differential scanning calorimetry

Analyses using differential scanning calorimetry (DSC) were carried out with a DSC-7 power compensation thermal analyzer (Perkin Elmer). Temperature calibration was performed with indium as a standard. Samples were placed in conventional aluminum pans and then heated under nitrogen flow at a scanning speed of 10 °C min^{-1} from 50 to 250 °C. Each sample (pure Trolox, T/MCM-41 complexes and physical mixture) was weighed to have the same amount of the guest.

2.2.4 FTIR spectroscopy

Fourier transform infrared spectra (FTIR) were recorded with a FTIR-5300 spectrometer (Jasco) equipped with a DTGS detector, working with resolution of 4 cm^{-1} over 32 scans. Samples were in the form of self-supporting pellets suitable for transmission infrared experiments and were placed in a quartz cell equipped with KBr windows, designed for RT studies in vacuum and controlled atmosphere. Before FTIR analysis the samples were outgassed at RT to remove physically adsorbed water and impurities.

2.2.5 Gas-volumetric analysis

Specific surface area (SSA), pore volume and size were measured by N_2 adsorption–desorption isotherms at -196 °C using gas-volumetric analyzer ASAP 2020 (Micromeritics). SSA was calculated using the Brunauer-Emmet-Teller (BET) method, average pore size and volume were calculated on the adsorption branch of the isotherms according to the Barrett-Joyner-Halenda (BJH) method (Kruk-Jaroniec-Sayari equations). Prior to analyses, samples were outgassed at RT overnight.

2.2.6 Gel and O/W emulsion preparation

The gel was prepared by simply mixing 2.0 g hydroxylethyl cellulose (HEC, ACEF) with 98.0 ml of pH 5.0 acetate buffer at about 80 °C. The resultant dispersion was mechanically stirred by a DLS stirrer (Velp Scientifica) until a gel was obtained and RT was reached. Thus pure Trolox or T/MCM-41 complexes, suspended in a small amount of pH 5.0 acetate buffer, were added to the dispersion systems.

The O/W emulsion was prepared by adding, under continuous homogenization by T25 Ultra-Turrax (IKA), the melted lipid phase composed of Phytocream 2000 (potassium palmitoyl hydrolyzed wheat protein and glyceryl stearate and cetearyl alcohol, Sinerga), Tegosoft EE (octyl octanoate, ACEF) and Abil 350 (dimethicone, ACEF) to an aqueous suspension of Carbopol ETD 2001 (carbomer, Biochim) and glycerol (ACEF) previously heated at 80 °C. After cooling to RT, Trolox, either as such or complexed with MCM-41, was added. The pH was adjusted to 5.0.

2.2.7 *In vitro* Trolox diffusion

Trolox diffusion from the different complexes was studied using an apparatus consisting of two horizontal glass cells, each of 23.0 ml volume, separated by a Spectra/Por (3500 Dalton MWCO) hydrophilic cellulose membrane (Spectrum Lab) with 4.5 cm^2 area. Trolox was employed

in pH 5.0 acetate buffer, in gel and in O/W emulsion, as a donor phase, either as such or included in MCM-41. Pure Trolox or T/MCM-41 complexes were added to the dispersion systems to get 1.7 mM Trolox. The receiving phase consisted of acetate buffer at 5.0 pH. The apparatus, sheltered from light, was maintained under stirring for 4 h period, during which at scheduled times of 30 min an aliquot of the receiving phase was withdrawn and analyzed using the HPLC method previously described. Each sample was prepared and analyzed in triplicate.

2.2.8 Photodegradation study

Irradiation tests were performed separately on pure Trolox and on T/MCM-41/DEG complex. The runs were carried out at pH 5.0 in the acetate buffer (0.25 mM Trolox), in the HEC gel (1.0 mM Trolox) and in the O/W emulsion (1.0 mM Trolox).

All the samples (10.0 ml) were placed at distance of 10.0 cm from a G40T10E UVB lamp (Sankyo Denki) with 2.5×10^{-4} W cm^{-2} power irradiance. During irradiation the samples were stirred by a RO 5 multiple magnetic stirrer (IKA). At scheduled times of 30 min, up to 3 h, a fixed amount of each sample was withdrawn for HPLC analysis and, in the case of the HEC gel and of the O/W emulsion, properly diluted with methanol. The study was carried out in triplicate.

2.2.9 Antiradical activity

The radical scavenging activity of free Trolox and Trolox/silica complex was determined by the $DPPH^{\bullet}$ free radical assay. Briefly, $DPPH^{\bullet}$ in its radical form absorbs at 525 nm but upon reduction by an antioxidant its absorption decreases. Equal aliquots (100.0 µL) of dilutions (within the range 0-400 µM) of Trolox or T/MCM-41/DEG complex in water/ethanol (85/15 v/v) were treated with 5.0 mL of 75.0 mM $DPPH^{\bullet}$ water/ethanol (50/50 v/v) solution. The absorbance of each reaction medium was spectrophotometrically monitored at 525 nm after 10 min of incubation under magnetic stirring to reach the steady-state condition.

The percentage of radical scavenging activity (% RSA) of Trolox in $DPPH^{\bullet}$ solution was calculated according Jang and Xu[26] using the following equation:

$$\% \text{ RSA} = [(A_0\text{-}A_1)/A_0] \times 100$$

where A_0 was the absorbance of $DPPH^{\bullet}$ at zero time and A_1 after 10 min of incubation for the reaction. Each sample was prepared and analyzed in triplicate and the percentage of radical scavenging activity was plotted against each dilution of Trolox.

3. Results and discussion

3.1 XRD

Low angle XRD patterns of the prepared complexes are shown in Fig. 1 with that of bare MCM-41 for comparison. The figure shows the typical (100), (110), (200) and (210) peaks, related to the ordered hexagonal (P6mm) network of mesopores. The last two peaks (200), (210) in particular testify of the long range order of the structure.

The peaks are maintained after Trolox inclusion, suggesting that the mesostructure is preserved. The main differences are in the peak intensity, which decreased with different extent in all complexes, particularly for the (110), (200) and (210) weak peaks. Moreover, a shift to higher angles is observed for sample T/MCM-41/W. Both phenomena (intensity decrease and peak shift) are usually taken as an indication for matter inclusion within the silica pores. This hypothesis will be supported by further analysis.

3.2 Thermo-gravimetric analysis

TGA was employed to measure the Trolox loading in the different complexes and to get information on its interaction with the silica surface. Fig. 2 reports TGA profiles of T/MCM-41 complexes (W, M, DEG and DRY), together with those of pure MCM-41 and Trolox, for comparison. As detailed in the experimental section, the experiments were carried out in nitrogen flow, which was changed to air at the end of the ramp, for an isotherm at 1000 °C. This last step

was necessary to quantify the amount of organic residues deposited on the silica surface during the pyrolysis process (vertical weight losses at 1000 °C in Fig. 2).

The Trolox decomposition profile (plotted in a different vertical scale for easier comparison) shows a first inflection around 194 °C, and a main weight loss at 277 °C (maximum of first derivative), both characterized by an exothermic nature (not reported). The former is consistent with DSC measurements (see below), being related to the Trolox melting point. The latter represents the thermal decomposition of the molecule.

All the T/MCM-41 complexes have a similar thermogram shape, so they will be discussed together. Firstly, bare MCM-41 showed a weight loss below 100 °C, typical of adsorbed water molecules, followed by a smooth weight decline up to 1000 °C, related to surface dehydroxylation.[27] This also holds for all complexes, which show additional weight losses around 350 and 440 °C, due to the thermal decomposition of adsorbed Trolox. The highest decomposition temperature with respect to free Trolox suggests an important stabilization effect of the inorganic matrix.

Trolox loading in each sample was estimated from the total weight loss, after subtraction of the alleged contribution from adsorbed water and dehydroxylation (the latter arbitrarily estimated from the weight loss in nitrogen in the 700–1000 °C range). The resulting values, listed in Table 1, suggest an effect of the solvent on the impregnation efficiency. The loading is in fact quite high in the complexes prepared with methanol as solvent and in that prepared by dry method with acetone. The results are in agreement with the loading calculated by spectrophotometric analysis after extraction with absolute methanol (see experimental section and corresponding column in Table 1). These values were double checked by measuring the Trolox amount remained in the supernatant (not reported).

3.3 Differential scanning calorimetry

DSC thermograms gave information about the interaction between Trolox and MCM-41. As shown in Fig. 3, the DSC curve of pure Trolox displays one endothermic peak at 195 °C (melting point) while the thermogram of MCM-41 does not show any peak. The disappearance of the Trolox melting peak in the thermogram of all the complexes is an indication of molecular dispersion of the guest in the matrix. In other words, Trolox is not present as solid state crystalline phase but we can infer that it is interacting molecularly with the silica surface. This is also true for sample T/MCM-41/DRY, where it would have been reasonable to expect re-crystallization of Trolox on the external surface of silica as a consequence of solvent evaporation.

On the contrary of the above, even if broadened and weaker the melting peak was detectable in the thermogram of the physical mixture Trolox/MCM-41 prepared at the same weight ratio of the complexes, as expected. However, the lower and slightly shifted peak suggests that a certain Trolox/silica interaction occurred also by simple physical mixture.

3.4 FTIR spectroscopy

Infrared analysis was carried out to check the structural integrity of Trolox molecules in the complexes and to gather information on their interaction with silica surface. In Fig. 4 (high and low frequency ranges, top and bottom respectively) the spectra obtained on samples T/MCM-41/DEG and T/MCM-41/DRY are compared with those of free Trolox, bare MCM-41 and of their physical mixture. The Infrared spectra of T/MCM-41/M and T/MCM-41/W samples, being qualitatively similar to that measured on T/MCM-41/DEG sample, are not reported for Fig. 4 clarity.

In the high energy range (top panel of Fig. 4) Trolox (curve d) was characterized by well defined absorptions, related to the OH and CH stretching modes (νOH and νCH, respectively). More in detail, the sharp and intense peak at 3550 cm^{-1} (shoulder at 3524 cm^{-1}) can be assigned to the νOH of unassociated phenol, while the weak band at 3386 cm^{-1} and the broad absorption in the 3300-2800 cm^{-1} interval are likely due to hydrogen bonded carboxylic groups.[28] In the lower energy range, νCH modes are related to unsaturated CH (3004 and 2988 cm^{-1}), saturated CH_2 (2936/2920

and 2837 cm^{-1}) and CH_3 moieties (2966 and 2888/2864 cm^{-1}) of the Trolox molecule. We can thus infer that Trolox molecules diluted in KBr are giving intermolecular hydrogen bonding through the carboxylic groups, while the phenol OH is protected by the steric hindrance of methyl groups.

As for the MCM-41 matrix, it is characterized by a band at 3746 cm^{-1}, with a component at 3720 cm^{-1} and a broad absorption between 3700 and 2800 cm^{-1}. These are due to Si-OH groups isolated (3746 cm^{-1}) and involved in hydrogen bonding as acceptor and donors, respectively.[29-31] Upon Trolox inclusion (T/MCM-41/DEG and T/MCM-41/DRY, curves b and c, respectively), the intensity of the band due to isolated Si-OH decreases, in favor of an increase in the broad absorption between 3700 and 2800 cm^{-1}, suggesting the formation of Si-OH/Trolox hydrogen bonded adducts. This effect is more evident for T/MCM-41/DEG complex, in minor amount on T/MCM-41/DRY and negligible in the physical mixture (curve e).

A further analysis of the high energy region clearly shows that Trolox is present on all complexes (including physical mixture), as testified by the complex νCH bands in the 3000-2800 cm^{-1} range. As for the νOH modes, the vibrational modes related to the carboxylic groups can not be appreciated, due to the strong absorption due to hydrogen bonding interaction with Si-OH. However, it is noticeable that the component at 3550 cm^{-1}, related to not interacting OH phenol groups in associated Trolox molecules (see above), can be clearly observed in both T/MCM-41/DRY and in physical mixture (curves c and e, respectively), but not in T/MCM-41/DEG (curve b). This suggests a different conformation of Trolox molecules in the complexes.

Additional information can be obtained by analysis of the low energy range (Fig. 4, bottom panel). The spectrum of Trolox in this region is dominated by the intense and narrow band at 1712 cm^{-1}, due to the νC=O of the carboxylic group. The relatively low position of the band (unassociated carboxylic groups are usually found at higher energy) is in good agreement with the hypothesis that it is in the form of hydrogen bonded intermolecular adducts.[28,32]

Other intense bands are found at 1454/1380 cm^{-1} (asymmetric and symmetric bending modes of CH_3, δ_{asym} and δ_{sym}, respectively), 1420 and 1355 cm^{-1}, assigned to the combination of δOH/νCO modes of carboxylic group and to the phenol δCOH, respectively. A component at 1626 cm^{-1}, which can be assigned to the aromatic νC=C mode,[28] is less intense. Trolox bands at lower frequency are not considered, since they are not visible in the silica complexes, due to the overlapping of the intense bulk silica modes.

In all the studied complexes, including physical mixture, the above described vibrational modes of Trolox are superimposed to the weak overtone/combination modes of the silica support. However, important differences can be observed upon inclusion, as described afterwards. Firstly, the νC=O band becomes broader and blue-shifted in the T/MCM-41/DEG and T/MCM-41/DRY complexes, showing a maximum at 1725 cm^{-1} (1720 cm^{-1} for T/MCM-41/DRY) and a shoulder at 1744 cm^{-1}, more intense in the former. In the physical mixture, on the contrary, the band shape resembles more that of free Trolox, though showing an additional component at 1734 cm^{-1}.

The position and shape of this band can be taken as an indication of the Trolox conformation in the different complexes. In fact, the significant blue-shift with respect to free Trolox, observed in both DEG and DRY complexes, indicates that the intermolecular interaction taking place in KBr, is not (or in minor amount) present within the silica pores. On the contrary, this interaction is still evident in the physical mixture, even if a minor fraction of molecules is probably interacting with the silica surface (shoulder at 1734 cm^{-1}). The broad character of the bands in both complexes testifies of a heterogeneous distribution of conformations.

Noticeably, the blue shift with respect to associated Trolox (spectrum in KBr) is larger on T/MCM-41/DEG sample with respect to T/MCM-41/DRY, suggesting a different conformation of molecules. Since in T/MCM-41/DEG (similarly to what observed in W and M samples, not reported for sake of clarity) the preparation method allowed for molecules diffusion inside the silica pores, we can thus infer that this kind of samples presents dispersed molecules in strong interaction

with the silica surface, giving a consistent blue-shift of the νC=O band with respect to associated molecules. On the contrary, kneading method is more likely to result in a large fraction of molecules filling the pores in associated form during the dry process. This should explain a νC=O band with intermediate position between T/MCM-41/DEG and physical mixture.

Other changes upon inclusion concern the νC=C band, which appears more intense and blue-shifted in T/MCM-41/DEG (from 1626 to 1636 cm^{-1}), while it is hardly noticeably in T/MCM-41/DRY and in the physical mixture. The interpretation of this change is not straightforward, since it is well known that the intensity of aromatic bands is strongly dependent on substitution and electronic effects, which could be affected by the interaction with the silica surface. Less evident changes can be found between 1500 and 1300 cm^{-1} region, particularly for the δOH/νCO combination modes and the phenol δCOH one.

Theoretical calculations could help to understand these results at a molecular level.[33] However, the measured spectra clearly enable us to highlight differences between DEG (taken as a model of the samples prepared by classical impregnation) and DRY complexes, suggesting a different distribution of Trolox molecules: mainly in the form of molecular hydrogen-bonded adducts with surface Si-OH in the former, and also present as intermolecular aggregates filling the pores opening, in the latter.

3.5 Gas-volumetric analysis

The low temperature adsorption/desorption isotherms of the different complexes are reported in Fig. 5 together with that of parent MCM-41. All curves present the type IV isotherm typical of mesoporous materials: the slope at intermediate p/p^0 (below 0.4) testifies of the capillary condensation of nitrogen inside the ordered mesopores while the type H1 hysteresis loop at high p/p^0 (> 0.90) is related to interparticle macroporosity.

By comparing curves from top to bottom it is possible to observe in all complexes a decrease in the slope related to mesopores, and a shift towards lower pressure values, indicating a shrinking of pores access which can be related to the Trolox inclusion. The trend is confirmed by the values summarized in Table 2 showing a substantial decrease of SSA, pore diameter and volume in all samples, though with different extent. In particular, the most drastic changes in all parameters for sample T/MCM-41/DRY are in agreement with the high Trolox loading and noteworthy decrease in XRD peaks intensity.

As for the high p/p^0 hysteresis loop, a closure with respect to bare MCM-41 is observed in all complexes. This corresponds to a decrease in the interparticle pore volume, to a major extent for samples T/MCM-41/M and T/MCM-41/DRY (see Table 2), and suggests Trolox inclusion also in this porosity. Notice that the measurement of the physical mixture indicates that both SSA and porosity are unaffected with respect to support (not reported).

3.6 *In vitro* Trolox diffusion

The employment of the *in vitro* transmembrane diffusion system is useful in the design and development of novel formulations. Recently, the Food and Drug Administration (FDA) has proposed that simple, porous synthetic membranes are suitable for assessing topical formulation as they act as a support yet are not rate limiting barriers.[34]

Results are summarized in Table 3 in terms of diffusion rate equations. Data indicate that in all the considered media the diffusion profile follows a pseudo-zero order kinetics for both pure Trolox and complexes. Furthermore, the diffusion from the complexes is delayed compared to that obtained from free Trolox confirming that a certain interaction between the two species occurred. Anyway the diffusion rate of Trolox from the complexes is quite evident confirming that no-covalent bonds (physical interactions) are involved in the complex formation.

It can be also observed that compared with simpler media (buffer and gel) the diffusion rates of Trolox - either free or complexed with MCM-41 - in O/W emulsion are slower, indicating that it

would part mainly at the O/W interface. Moreover, T/MCM-41/M and T/MCM-41/DEG in emulsion show the slowest diffusion suggesting that reducing the presence of water in the preparation method might favor the inclusion of Trolox inside the silica pores. A separate discussion may be made for T/MCM-41/DRY complex that presents the highest rate diffusion (especially in HEC gel and in O/W emulsion). As discussed in previous section, it can be hypothesized that in this case a large fraction of molecules are filling the mesopores in the form of intermolecular aggregates. In this conformation, the hydrogen bonding interaction with Si-OH should be weaker, thus explaining the quicker release.

3.7 Photodegradation study

Trolox displays a peak around 290 nm, the intensity of which decreases upon irradiation as already observed in our previous work.[35] Accordingly, in this study UV detection by HPLC analysis of intact Trolox revealsa mean retention time of 4.30 min. Under UVB light it degrades in all the tested media, probably by a mechanism of photooxidation, and photosensitizers were not necessary. The degradation is followed by a progressive decrease in peak area at the above mentioned retention time and in parallel, from 90 min of irradiation, by the appearance of a secondary peak around 4.90 min that can be attributed to a product of degradation. On the basis of literature data[36] and of our previous reports[35] it can be reasonably assumed that a conversion of Trolox to Trolox-C-quinone occurred. This degradation phenomenon is typical of lipoperoxidation reactions and proceeds with the involvement of oxygen as a partner of reaction. This drawback is avoided by acting on the polarity of the dispersion medium because a more apolar environment can inhibit oxidative processes.

In this work, the Trolox photodegradation was studied on sample T/MCM-41/DEG, taken as a representative example of good compromise between Trolox loading, release kinetics and molecular dispersion within the pores. Interestingly, our results indicate that in O/W emulsion after 180 min of UVB irradiation the percentage of degraded Trolox is just 39.5% of initial concentration

meanwhile in aqueous systems Trolox is almost completely degraded (in acetate buffer 100%, in HEC gel 90.5%). Data confirm that passing from a less polar medium to a more polar one, the photodegradation rate of Trolox increases. Trolox UV photodegradation is thus limited, but not eliminated, when passing from aqueous solutions and HEC gel to O/W emulsion, system more representative of actual topical formulations. The approach to this problem thus implies the use of carrier systems that can slow down degradation.

As mentioned above, complexes with cyclodextrins were developed in our laboratory to increase the stability of Trolox.[5,6] Unfortunately, we discovered that hosting molecules can reduce but not completely eliminate Trolox degradation. In this report we propose MCM-41 as protective agent since its internal surface can serve as a microenvironment in which molecules can be loaded and protected from external injury. In addition, Ambrogi and co-workers[12] discovered that the inclusion of some UV ray absorbents in the MCM-41 framework can affect their stability. Similarly here, we examine the possibility of increasing Trolox photostability by complexing it with MCM-41. Photodegradation straight lines of Trolox and T/MCM-41/DEG in the selected media are shown in Fig. 6, while Table 4 reports the photodegradation equations. Results evidence that the general equation of the reported lines is

$$C_t/C_0 \times 100 = - kt$$

where C_0 is the initial concentration of Trolox, C_t is the Trolox concentration after a given irradiation time (t) and k is the kinetic constant of the reaction. The percentage values are plotted *vs* UVB irradiation time expressed in min.

Equations also show that both free Trolox and T/MCM-41/DEG follow a pseudo-zero order photodegradation kinetics in all the selected media. The kinetic constants of complex are lower indicating a protective action of MCM-41 towards Trolox UVB photodegradation. Summarizing, the degradation rate of Trolox decreases when it is included into the silica framework regardless of the medium in which the complex is dispersed. Furthermore, results of Table 4 indicate a certain influence of the dispersion medium on the photostability also for the complex.

On the other hand, in our above cited previous reports, Trolox/cyclodextrins complexes showed a photodegradation pseudo-zero order kinetics with a rate directly dependent on the polarity of the dispersion medium. Particularly, the efficiency of cyclodextrin inclusion in increasing Trolox photostability followed this sequence: O/W emulsion>HEC gel>aqueous solution. Similarly, in this case the best results are obtained with emulsion system, thus it can be reasonably supposed that both free Trolox and T/MCM-41/DEG were confined at the O/W interface. These findings demonstrate that mesoporous matrix together with an apolar environment should significantly reduce the photooxidative reactions.

3.8 Antiradical activity

The reaction with $DPPH^{\bullet}$ is widely used in assessing the ability of antioxidants to transfer labile atoms to radicals. This assay is based on the reduction of $DPPH^{\bullet}$ which causes an absorbance decrease at 525 nm after acceptance of an electron or hydrogen radical from an antioxidant compound. Accordingly, in this study the antioxidant activity of Trolox was evaluated from the remaining $DPPH^{\bullet}$ when the kinetics reached the steady-state as a function of the molar antioxidant concentration. This test was performed on pure Trolox and on T/MCM-41/DEG, arbitrarily selected as discussed above. Fig. 7 illustrates that the scavenging effect (% RSA) of Trolox increased with its concentration. Furthermore, the % RSA of the complex was comparable to that observed with pure Trolox confirming that the molecule structure was preserved in the complex, as already assessed by FTIR analysis and it was available for interaction with $DPPH^{\bullet}$.

4. Conclusions

Trolox compound was employed as a case study to test the potentiality of MCM-41 mesoporous silica as carrier for topical application, by preparing T/MCM-41 complexes. Different inclusion methodologies were employed, varying solvent (water, methanol, acetone), procedure

(classical impregnation or kneading method) and pretreatment of the silica matrix (preliminary outgassing to remove water adsorbed on the pore surface).

TGA shows the inclusion of a good amount of Trolox in all complexes, increasing in the order: W < DEG < M < DRY, suggesting an important effect of the solvent on the final loading. Physico-chemical characterization indicates that Trolox molecules are mainly included inside the silica pores, as testified by modification of XRD and DSC peaks, and by the decrease of specific surface area, pore volume and diameter upon inclusion.

Further information on the host/guest interaction could be obtained by FTIR spectroscopy, by analyzing modifications in the typical vibrational modes of silica and Trolox as a result of their interaction. This analysis was focused on samples T/MCM-41/DEG (taken as representative example of samples prepared by classical impregnation) and T/MCM-41/DRY complexes, compared to physical mixture and pure compounds as references. The typical Trolox modes were observed in all complexes testifying of the structure preservation. However, some bands were particularly affected by inclusion, in different way/extent on the two selected samples. Namely, the narrow peak at 3550 cm^{-1}, assigned to unperturbed phenol νOH groups in intermolecularly associated Trolox molecules, was present on T/MCM-41/DRY sample but not on T/MCM-41/DEG. Moreover, the strong band related to the carboxylic νC=O groups (at 1712 cm^{-1} in pure Trolox) was broadened and blue-shifted in both complexes, but in larger amount in T/MCM-41/DEG. These changes, coupled to a higher degree on hydrogen bonding (broad absorption between 3700 and 2800 cm^{-1}), suggest a more efficient molecular dispersion on the samples prepared by impregnation (T/MCM-41/DEG) with respect to the one prepared by rapid solvent evaporation (T/MCM-41/DRY).

When their performances in different dispersion media (acetate buffer, gel and O/W emulsion) were tested, the T/MCM-41 complexes showed a slower diffusion compared to the free Trolox, particularly for T/MCM-41/M and T/MCM-41/DEG in O/W emulsion. In addition to FTIR data, such result suggests a better inclusion of Trolox in these complexes with respect to T/MCM-

41/DRY, where a fraction of guest molecules could be filling the mesopores in the form of intermolecular aggregates, thus resenting a weaker interaction with the silica surface.

Finally, T/MCM-41/DEG was tested for photodegradation studies in the three selected media and about its antiradical activity in comparison to the free compound. Results showed an effect of the silica matrix in stabilizing Trolox toward UVB induced photodegradation, while maintaining its antiradical activity. Moreover, photostability was particularly improved in the O/W emulsion, where it can be supposed that both Trolox and T/MCM-41 complex were confined at the O/W interface. This is a promising result for topical application, since O/W emulsions are widely employed in pharmaceutical formulations.

Acknowledgments

Compagnia di San Paolo and University of Turin are gratefully acknowledged for funding Project ORTO114XNH through "Bando per il finanziamento di progetti di ricerca di Ateneo - anno 2011". Prof. S. Coluccia and Prof. M.E. Carlotti are gratefully acknowledged for fruitful discussion.

Figure captions

Fig. 1. Powder XRD patterns of: a) MCM-41; b) T/MCM-41/W; c) T/MCM-41/DEG; d) T/MCM-41/DRY.

Fig. 2. TGA profiles of: a) bulk MCM-41; b) T/MCM-41/W; c) T/MCM-41 DEG; d) T/MCM-41/M; e) T/MCM-41/DRY. Decomposition profile of pure Trolox is reported, in different vertical scale for easier comparison.

Fig. 3. DSC thermograms of pure Trolox, physical mixture, MCM-41 and T/MCM-41 complexes.

Fig. 4. FTIR spectra of: a) MCM-41; b) T/MCM-41/DEG; c) T/MCM-41/DRY; d) free Trolox; e) corresponding physical mixture, in the high and low frequency ranges (top and bottom respectively).

Fig. 5. Nitrogen isotherm adsorption (□) and desorption (×) on: a) MCM-41; b) T/MCM-41/W; c) T/MCM-41/DEG; d) T/MCM-41/M; e)T/MCM-41/DRY.

Fig. 6. Time evolution of free Trolox (black) and T/MCM-41/DEG (grey) under UVB irradiation in acetate buffer (solid line, diamond), HEC gel (dotted line, square) or O/W emulsion (dotted and dashed line, circle), at pH 5.0.

Fig. 7. Antiradical activity (expressed as % RSA) of free Trolox and T/MCM-41/DEG towards $DPPH^{\bullet}$. Each bar represents the means ± SD obtained in three independent experiments (n=3).

Figure 1

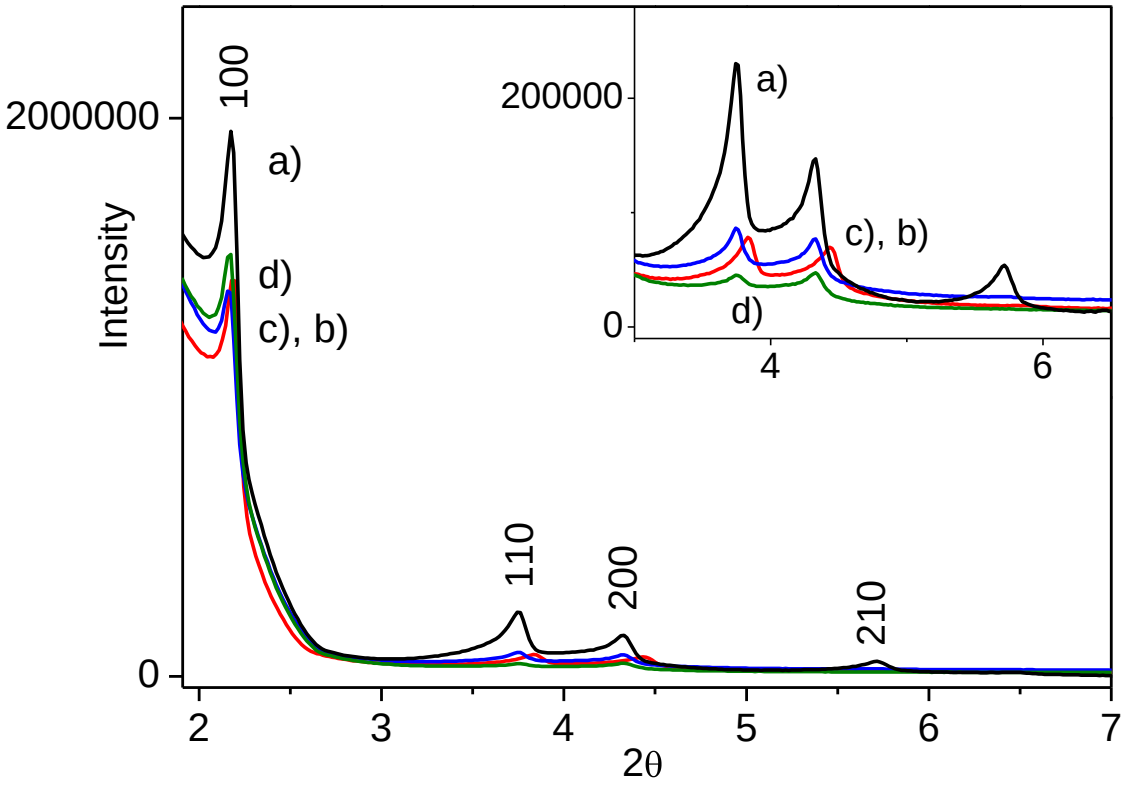
2000000
0
Intensity
100
a)
d)
c), b)
110
200
210
2
3
4
5
6
7
2θ
200000
0
a)
c), b)
d)
4
6

Figure 2

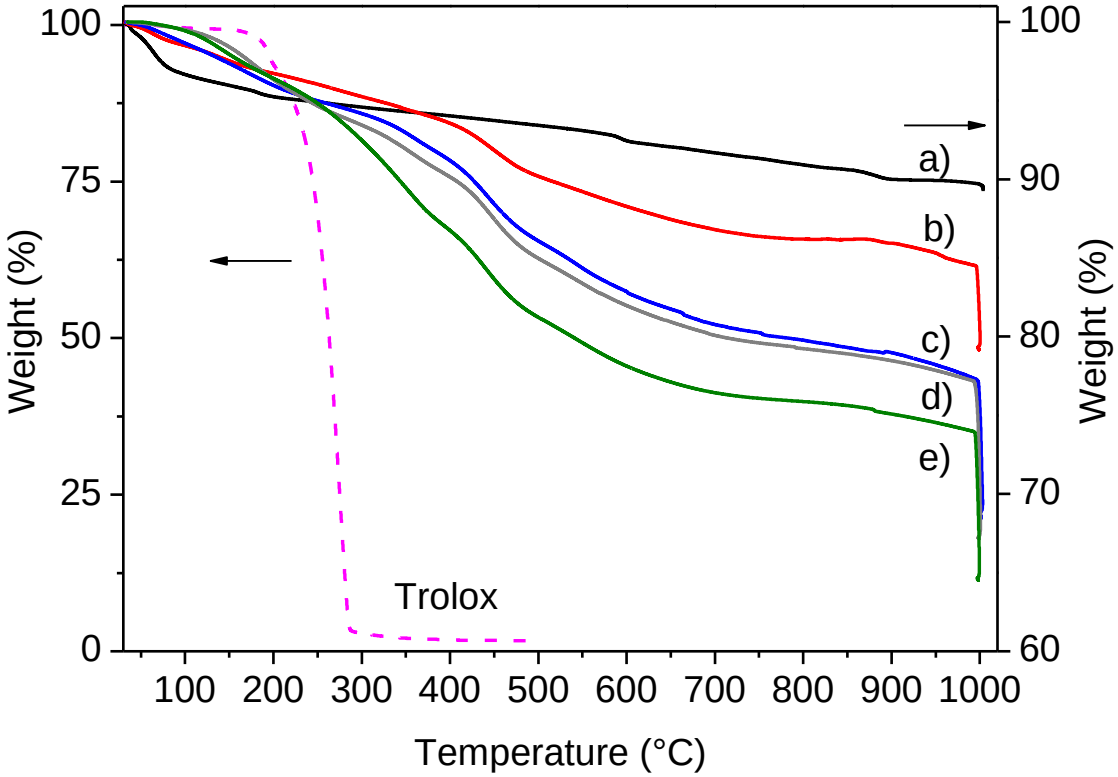
100
75
50
25
0
Weight (%)
100
90
80
70
60
Weight (%)
a)
b)
c)
d)
e)
Trolox
100 200 300 400 500 600 700 800 900 1000
Temperature (°C)

Figure 3

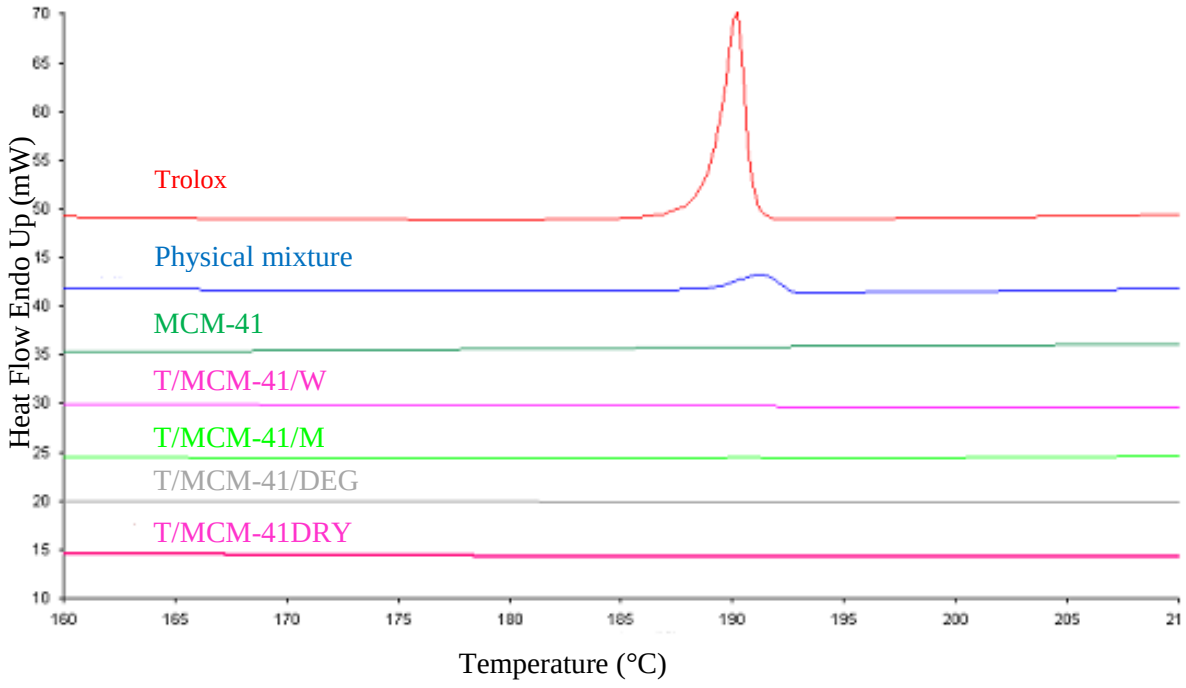
Heat Flow Endo Up (mW)
70
65
60
55
50
45
40
35
30
25
20
15
10
Trolox
Physical mixture
MCM-41
T/MCM-41/W
T/MCM-41/M
T/MCM-41/DEG
T/MCM-41DRY
160
165
170
175
180
185
190
195
200
205
21
Temperature (°C)

Figure 4 top

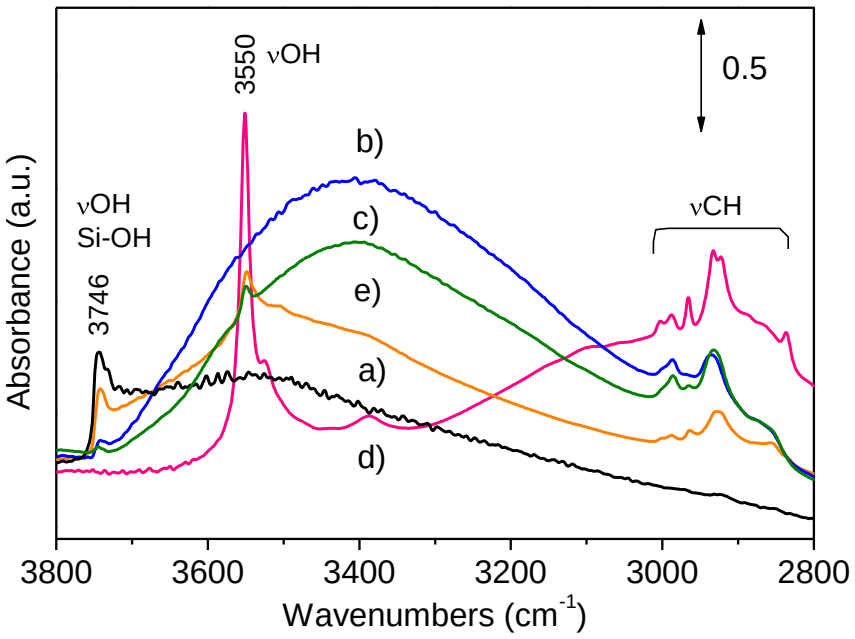

Figure 4 bottom

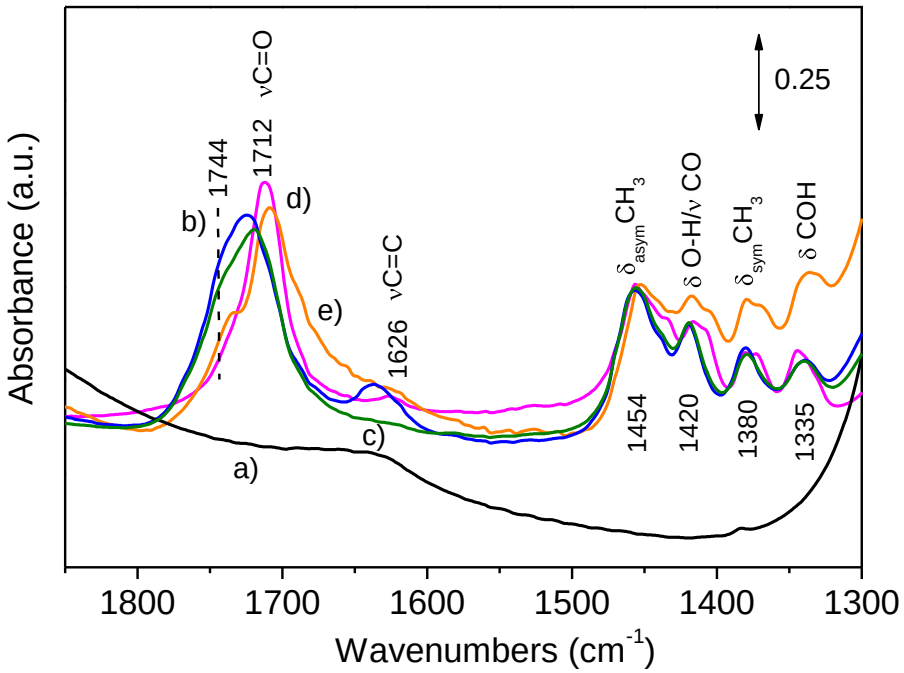

Figure 5

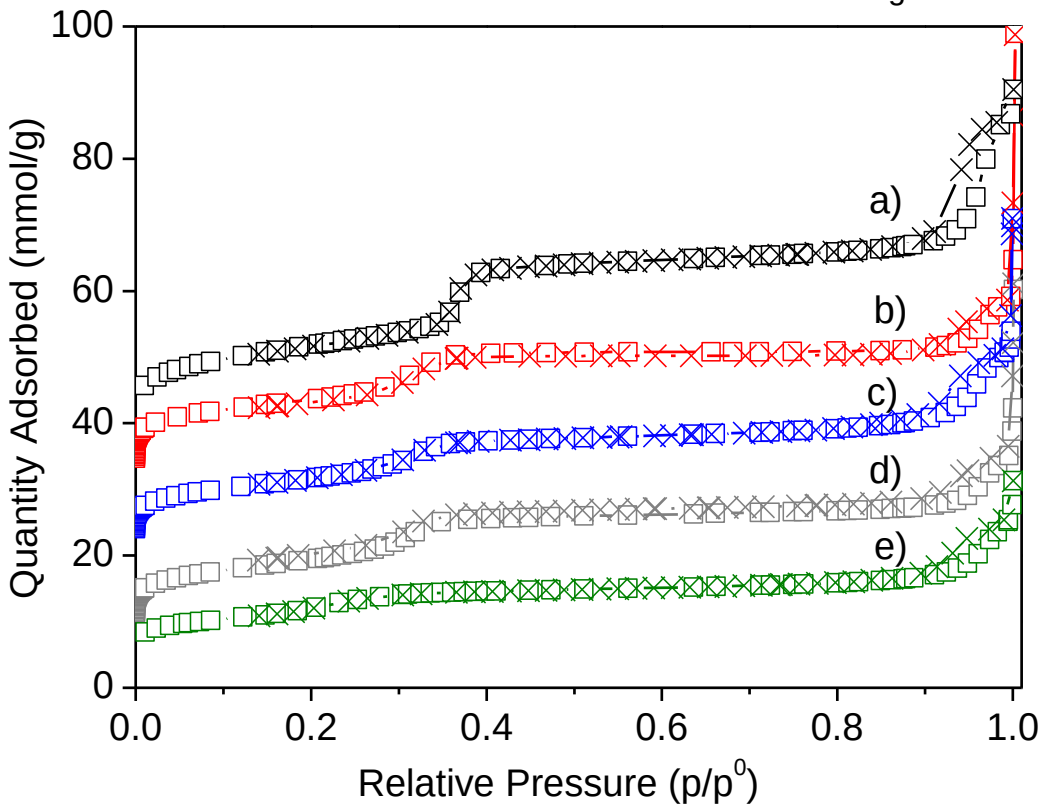
Quantity Adsorbed (mmol/g)
Relative Pressure (p/p0)
0
20
40
60
80
100
0.0
0.2
0.4
0.6
0.8
1.0
a)
b)
c)
d)
e)

Figure 6

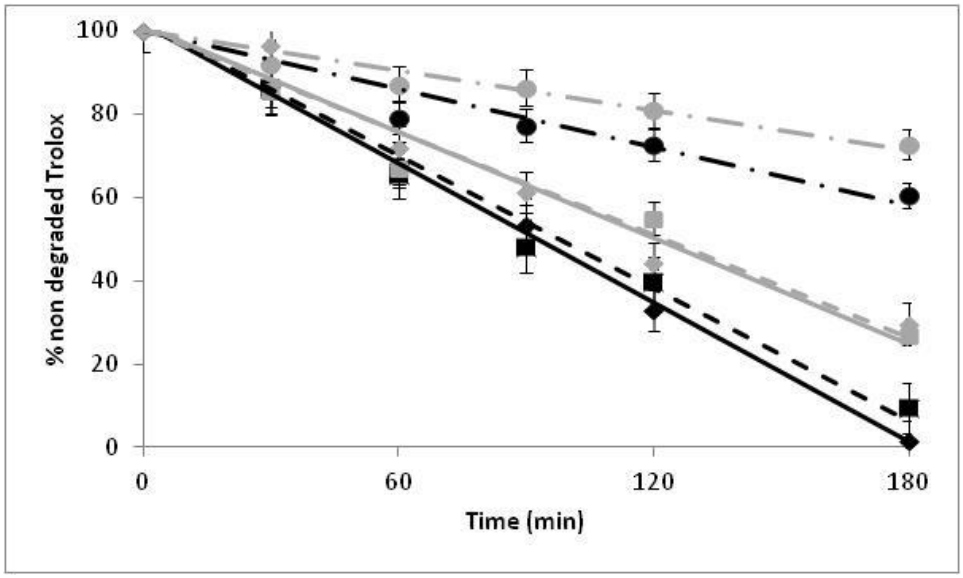

Figure 7

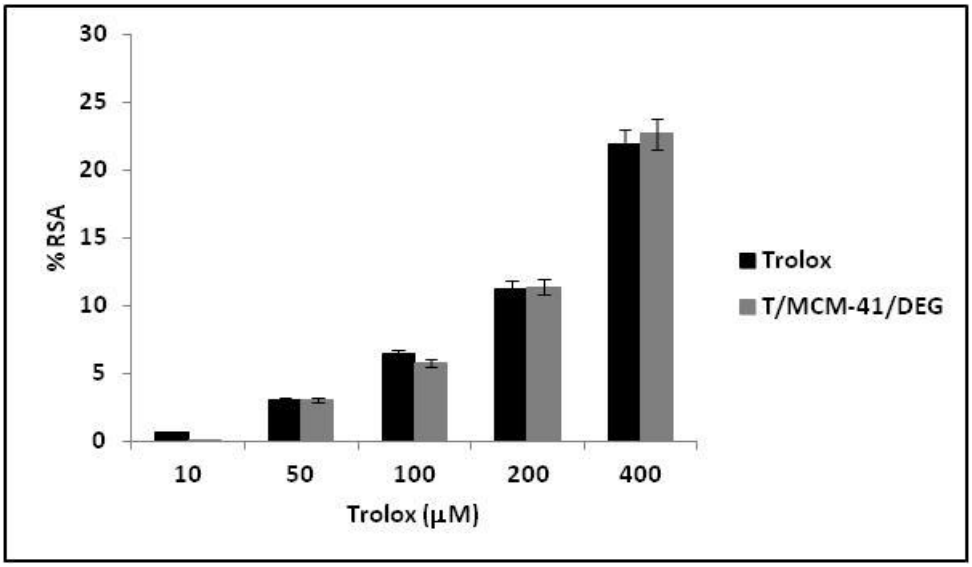
30
25
20
15
10
5
0
% RSA
10
50
100
200
400
Trolox (μM)
Trolox
T/MCM-41/DEG

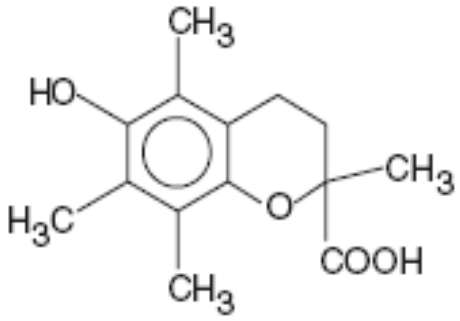

Scheme 1: Structure of Trolox molecule

Table 1 Percentage weight loss from TGA and percentage of loading from spectrophotometric analysis

Samples	Water [a]	Hydroxyl groups [b]	Trolox	
			TGA [c]	UV-Vis [d]
MCM-41	3.4	7.2	-	-
T/MCM-41/W	1.6	2.4	17.1	16.7
T/MCM-41/DEG	1.4	3.3	26.4	25.2
T/MCM-41/M	0.5	2.9	29.2	28.0
T/MCM-41/DRY	0.5	2.4	32.6	30.1

[a] Measured in the 30-100 °C range; [b] measured in the 700-1000°C range, before isotherm in air; [c] remaining weight loss other than [a] and [b]; [d] spectrophotometric analysis after extraction with absolute methanol

Table 2 Porosity and specific surface area of the silica based samples

Samples	SSA [a] ($m^2 g^{-1}$)	Pore diameter [a] (Å)	Pore volume [c] ($cm^3 g^{-1}$)	Pore volume [d] ($cm^3 g^{-1}$)
MCM-41	1081	38	0.88	0.58
T/MCM-41/W	645	36	0.48	0.33
T/MCM-41/M	714	35	0.56	0.23
T/MCM-41/DEG	658	36	0.49	0.36
T/MCM-41/DRY	551	30	0.30	0.23

[a] Calculated by the BET method; [b] mean pore diameter calculated by BJH method in the adsorption branch, employing the Kruk-Jaroniec-Sayari model; [c] and [d] calculated by BJH method in the 25–50 Å and 200–1000 Å ranges, respectively.

Table 3 Diffusion rate equations of Trolox and T/MCM-41 complexes through a cellulose membrane

Samples	Acetate buffer	HEC gel	O/W emulsion
Trolox	$y = 0.1540x$ $R^2 = 0.9953$	$y = 0.1903x$ $R^2 = 0.9669$	$y = 0.1324x$ $R^2 = 0.9667$
T/MCM-41/W	$y = 0.1204x$ $R^2 = 0.9683$	$y = 0.1544x$ $R^2 = 0.9655$	$y = 0.0883x$ $R^2 = 0.9764$
T/MCM-41/M	$y = 0.1161x$ $R^2 = 0.9856$	$y = 0.1450x$ $R^2 = 0.9916$	$y = 0.0678x$ $R^2 = 0.9540$
T/MCM-41/DEG	$y = 0.1279x$ $R^2 = 0.9946$	$y = 0.1497x$ $R^2 = 0.9721$	$y = 0.0640x$ $R^2 = 0.9892$
T/MCM-41/DRY	$y = 0.1228x$ $R^2 = 0.9714$	$y = 0.1648x$ $R^2 = 0.9770$	$y = 0.0887x$ $R^2 = 0.9896$

Table 4 Degradation rate equations of Trolox and T/MCM-41/DEG under UVB irradiation in acetate buffer, HEC gel or O/W emulsion, at pH 5.0

Media	Trolox	T/MCM-41/DEG
Acetate buffer	y= -0.5453x+100 R^2=0.9695	y= -0.4298x+100 R^2=0.9009
HEC gel	y= -0.5013x+100 R^2=0.9256	y= -0.4210x+100 R^2=0.9661
O/W emulsion	y= -0.2339x+100 R^2=0.9238	y= -0.1588x +100 R^2=0.9209

References

1 T. Saito, N. A. Hartell, H. Muguruma, S. Hotta, S. Sasaki, M. Ito and I. Karube, *Photochem. Photobiol.,* 1998, **68**, 745-748.

2 D. J. Hubert, A. Dawe, N. T. Florence, K. D. W. F. Gilbert, T. N. Angele, D. Buonocore, P. V. Finzi, G. Vidari, N. T. Bonaventure, F. Marzatico and M. F. Paul, *Inflammopharmacol.,* 2011, **19**, 35-43.

3 M. Lopez, F. Martinez, C. Del Valle, M. Ferrit and R. Luque, *Talanta,* 2003, **60**, 609-616.

4 K. Satoh, T. Kadofuku and H. Sakagami, *Anticancer Res.,* 1997, **17**, 2459-2463.

5 M. E. Carlotti, S. Sapino, S. Marino, E. Ugazio, F. Trotta, D. Vione, D. Chirio and R. Cavalli, *J. Inclusion Phenom. Macrocyclic Chem.,* 2008, **61**, 279-287.

6 S. Sapino, M. Trotta, G. Ermondi, G. Caron, R. Cavalli and M. E. Carlotti, *J. Inclusion Phenom. Macrocyclic Chem.*, 2008, **62**, 179-186.

7 M. E. Carlotti, S. Sapino, E. Ugazio and G. Caron, *J. Inclusion Phenom. Macrocyclic Chem.*, 2011, **70**, 81-90.

8 M. E. Carlotti, S. Sapino, R. Cavalli, M. Trotta, F. Trotta and K. Martina, *J. Inclusion Phenom. Macrocyclic Chem.*, 2007, **57**, 445-450.

9 S. Sapino, M. E. Carlotti, R. Cavalli, M. Trotta, F. Trotta and D. Vione, *J. Inclusion Phenom. Macrocyclic Chem.*, 2007, **57**, 451-455.

10 U. Costantino, V. Ambrogi, M. Nocchetti and L. Perioli, *Microporous Mesoporous Mater.*, 2008, **107**, 149-160.

11 Y. Kohno, K. Totsuka, S. Ikoma, K. Yoda, M. Shibata, R. Matsushima, Y. Tomita, Y. Maeda and K. Kobayashi, *J. Colloid Interface Sci.,* 2009, **337**, 117-121.

12 V. Ambrogi, L. Perioli, F. Marmottini, L. Latterini, C. Rossi and U. Costantino, *J. Phys. Chem. Solids,* 2007, **68**, 1173-1177.

13 Y. Kohno, S. Tsubota, Y. Shibata, K. Nozawa, K. Yoda, M. Shibata and R. Matsushima, *Microporous Mesoporous Mater.,* 2008, **116**, 70-76.

14 T. Itoh, K. Yano, Y. Inada and Y. Fukushima, *J. Am. Chem. Soc.*, 2002, **124**, 13437-13441.

15 O. A. Kazakova, V. M. Gun'ko, N. A. Lipkovskaya, E. F. Voronin and V. K. Pogorelyi, *Colloid J.*, 2002, **64**, 412-418.

16 T. V. Fedyanina, V. N. Barvinchenko, N. A. Lipkovskaya and V. K. Pogorelyi, *Colloid J.*, 2008, **70**, 215-220.

17 M. Vallet-Regi, F. Balas and D. Arcos, *Angew. Chem. Int. Edit.*, 2007, **46**, 7548-7558.

18 S. Wang, *Microporous Mesoporous Mater.*, 2009, **117**, 1-9.

19 M. Hartmann, *Chem. Mater.*, 2005, **17**, 4577-4593.

20 H. H. P. Yiu and P. A. Wright, *J. Mater. Chem.*, 2005, **15**, 3690-3700.

21 Y. Wang, A. D. Price and F. Caruso, *J. Mater. Chem.*, 2009, **19**, 6451-6464.

22 M. Manzano, V. Aina, C. O. Arean, F. Balas, V. Cauda, M. Colilla, M. R. Delgado and M. Vallet-Regi, *Chem. Eng. J.*, 2008, **137**, 30-37.

23 J. S. Beck, J. C. Vartuli, W. J. Roth, M. E. Leonowicz, C. T. Kresge, K. D. Schmitt, C. T. W. Chu, D. H. Olson and S. E. W., *J. Am. Chem. Soc.*, 1992, **114**, 10834-10843.

24 C. T. Kresge, M. E. Leonowicz, W. J. Roth, J. C. Vartuli and J. S. Beck, *Nature*, 1992, **359**, 710-712.

25 N. V. Roik and L. A. Belyakova, *J. Mol. Struct.*, 2011, **987**, 225-231.

26 S. Jang and Z. Xu, *J. Agric. Food. Chem.*, 2009, **57**, 858-862.

27 S. A. Kozlova and S. D. Kirik, *Microporous Mesoporous Mater.*, 2010, **133**, 124-133.

28 G. Socrates, *Infrared and Raman characteristic group frequencies*; Third edition ed.; John Wiley & Sons Ltd: Chichester, England, **2006**.

29 A. Zecchina, S. Bordiga, G. Spoto, L. Marchese, G. Petrini, G. Leofanti and M. Padovan, *J. Phys. Chem.*, 1992, **96**, 4985-4990.

30 S. Tosoni, B. Civalleri, F. Pascale and P. Ugliengo, *J. Phys.: Conf. Ser.*, 2008, **117** 1-8.

31 I. Braschi, G. Gatti, B. C., G. Berlier, S. V., M. Cossi and L. Marchese, *J. Phys. Chem. C*, 2012.

32 A. J. Collins and K. J. Morgan, *J. Chem. Soc.*, 1963, 3437-3440.

33 A. Rimola, M. Sodupe, S. Tosoni, B. Civalleri and P. Ugliengo, *Langmuir,* 2006, **22**, 6593-6604.

34 N. G. Shiow-Fern, J. Rouse, D. Sanderson and G. Eccleston, *Pharmaceutics,* 2010, **2**, 209-223.

35 M. E. Carlotti, S. Sapino, D. Vione, E. Pelizzetti and M. Trotta, *J. Dispersion Sci. Technol.,* 2004, **25**, 193-207.

36 M. Nakamura and T. Hayashi, *Arch. Biochem. Biophys.*, 1992, **299**, 313-319.